

Fig. 2 Return flux impacts for outgassing species—BGK model—full surface accommodation.

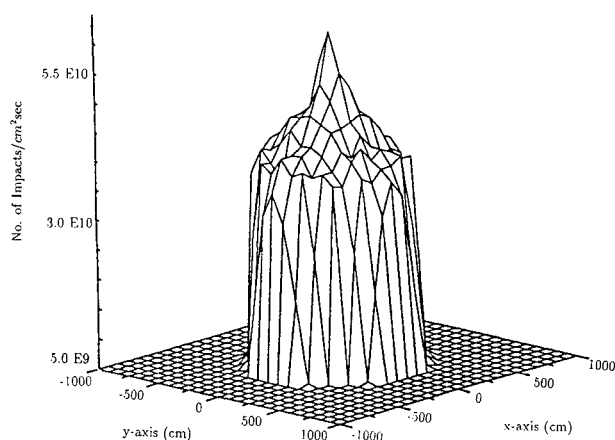


Fig. 3 Return flux impacts for outgassing species—full flow model—full surface accommodation.

return flux conditions, the MOLFLUX code was run for the CO_2 return flux conditions. These results are shown in Figs. 1 and 2 for both reduced and full surface accommodation conditions. The peak values for both surface conditions was approximately 3.2×10^8 impacts/cm²/s. Unlike the ambient species results, the return flux distribution peaked at the center of the disk and decreased rapidly toward the edges. The CARLOS code, representing the full physics of the problem, was next run for the CO_2 return flux case with full surface accommodation. The results of this run are shown in Fig. 3. The peak value of the return flux contact is 7.0×10^{10} impacts/cm²/s and occurs at the center of the disk with a decrease toward the disk edge not as severely pronounced as the BGK results. It is noted that the peak value of the full physics result is approximately 200 times that of the BGK result.

It is expected that the recontact distribution should be axisymmetric over the surface of the disk. Our calculations (not shown herein) have shown that the freestream contact distribution is essentially uniform over the surface. This result is taken as another indication that these calculations represent a physically realistic description of the problem.

Conclusions

It is evident that the use of a BGK-based model for this outgassing problem underpredicts the return flux by roughly two orders of magnitudes compared to a DSMC-based model that used the largest molecular diameters found in the literature. However, the results obtained from either of these models have not yet been validated under actual flow conditions.

The BGK-based method is a neutrals-only simulation scheme. It does not have the capability, as does the full flow simulation, of representing the remaining fully coupled effects (such as plasma flow, the electromagnetic field effects, and spacecraft charging) in addition to the neutral particle flow. The exclusion of all but the neutral flow, along with the BGK simplification, apparently makes the BGK method inadequate to represent the return flux problem properly.

This study has also indicated that surface accommodation has a negligible effect on the computed return flux.

No orbital experiment to date has had sensors of sufficient sensitivity to yield compelling data. The physical phenomena that require assumptions on the part of computational investigators remain a major restriction to this area of investigation. Specifically, the physical processes involved in the gas-gas interaction as well as gas-surface interaction require a better understanding. Upcoming NASA Shuttle missions should provide some of this data.

Acknowledgments

The investigators would like to thank NASA/JSC for its support, especially Max Engert of the Engineering Directorate for making available the Engineering Computational Facility, and Rose Rodriguez of LESC for making the MOLFLUX runs used in this study.

References

- ¹Justiz, C. R., Sega, R. M., Dalton, C., and Ignatiev, A., "A Hybrid Flow Model for Charged and Neutral Particles Around Spacecraft in Low Earth Orbit," AIAA Paper 92-2935, July 1992.
- ²Bartel, T. J., Blackwell, B. F., and Sheldal, R. E., "Measurement of the Free Stream Density for Re-Entry Vehicles: A Design Study," *Proceedings of the 17th International Symposium on Rarefied Gas Dynamics*, edited by A. E. Beylich, Aachen, 1990, pp. 1474–1481.
- ³Bartel, T. J., and Hudson, M. L., "Energy Accommodation Modeling of Rarefied Flow over Re-Entry Geometries Using DSMC," AIAA Paper 89-1879, July 1989.
- ⁴Bird, G. A., *Molecular Gas Dynamics*, Clarendon Press, Oxford, England, UK, 1976.
- ⁵Bird, G. A., "Monte Carlo Simulation in an Engineering Context," *12th International Symposium on Rarefied Gas Dynamics*, Vol. 74, Progress in Astronautics and Aeronautics, AIAA, New York, 1981.
- ⁶Rios, E. R., and Rodriguez, R. T., *Molecular Flux User's Manual*, NASA-JSC-22496, Rev. 1; Feb. 1989.
- ⁷Justiz, C. R., "Wake Characterization: Full Flow Simulation of Space Structures in Low Earth Orbit," Ph.D. Dissertation, Univ. of Houston, Houston, TX, 1991.

Thermophysical Properties of Cyclotrimethylenetrinitramine

Martin S. Miller*

U.S. Army Research Laboratory,
Aberdeen Proving Ground, Maryland 21005

Introduction

Thermal properties of pure nitramines are of considerable interest to the energetic-materials community, yet accurate measurements of these properties are nontrivial and

Received Nov. 22, 1993; revision received April 5, 1994; accepted for publication April 11, 1994. This paper is declared a work of the U.S. Government and is not subject to copyright protection in the United States.

*Research Physicist, Weapons Technology Directorate.

almost nonexistent in the open literature. Propellants and plastic-bonded explosives typically contain more than a two-thirds mass fraction of cyclotrimethylenetrinitramine (RDX) or cyclotetramethylenetetranitramine (HMX). Because the individual crystals in these composites are randomly oriented relative to one another, there is a particular need for thermal properties of these nitramines in polycrystalline form. This Note reports simultaneous measurements of the thermal conductivity and thermal diffusivity of pressed-powder specimens of RDX using a technique recently developed for small test specimens of energetic materials.¹ These data were obtained for specimen temperatures ranging approximately between -20 and $+50^{\circ}\text{C}$.

Experimental

The technique used is fully described in Ref. 1, but a brief summary is provided here for convenience. The experimental setup is designed to provide a close approximation to the mathematically ideal case of a step-function heat flux emanating from the planar boundary between two semi-infinite solids. Experimentally, the heat flux is generated by the sudden onset of resistive heating of a $5\text{-}\mu\text{m}$ -thick Constantan[®] foil. Due to the finite heat capacity of the foil, a nonideal step-function heat flux is produced by a step-function current in the foil. The extent to which measurements of the diffusivity are affected by this nonideality has been determined.² Under the conditions reported here, the resulting error is less than 2.5%. The test specimen approximates one of the two semi-infinite solids, and a material of known thermal properties (polymethylmethacrylate) approximates the other. Under present conditions, the finite thickness of the specimen contributes less than 1% error to the reported measurements. The test specimen consists of two separate parts, a wafer 0.7 mm thick by 6 mm diam, and a "backup" piece 6.5 mm long by 6 mm diam. Between these two specimen parts a $5\text{-}\mu\text{m}$ -thick Chromel/Alumel[®] foil-type thermocouple is interposed. After the sudden onset of the heat flux, the temperature between the two specimen pieces is measured for a period of about 4 s and compared to the exact solution of the idealization. Values of the diffusivity and conductivity are found by a nonlinear, least-squares fit of the solution to the data. The overall accuracy of the method is estimated to be about 5%.

The test fixture described in Ref. 1 consists of a cylindrical copper block with voids suitably milled from the interior to provide support for the foil, specimen, and thermocouple. Although the original description of the technique was confined to ambient laboratory temperature, copper was used in anticipation of the need to equilibrate the specimen rapidly to various temperatures and to provide a uniform-temperature surround for the specimen in order to measure thermal properties at different temperatures. Temperature control of the specimen was achieved by soldering copper tubing to the exterior of the fixture and fitting it with a mineral-fiber insulation jacket. A 50% ethylene glycol mixture with water was then circulated through the tubing from a temperature-controlled reservoir. Auxiliary experiments were performed to determine the time needed for the fixture to reach various steady-state temperatures before testing could begin.

The RDX powder used in this study was obtained from Waltham Abbey, England, and was of higher purity than the U.S. military grade. High pressure liquid chromatography (HPLC) analysis revealed it to have a 1% HMX impurity. The wafer and backup piece were formed separately by pressing in a steel die to about 95% of maximum theoretical density (TMD). After pressing, the specimen pieces were desiccated for several weeks prior to testing.

Results

Tests were performed at four temperatures, spanning the approximate range of -20°C to $+50^{\circ}\text{C}$. The averages and

Table 1 Measured thermophysical properties of polycrystalline RDX

Temperature, K	$10^4 \times$ Thermal conductivity, $\text{cal/cm-s-}^{\circ}\text{C}$	$10^3 \times$ Thermal diffusivity, cm^2/s
255	4.74 ± 0.22	1.32 ± 0.04
276	5.44 ± 0.28	1.32 ± 0.04
295	4.62 ± 0.34	1.08 ± 0.05
320	4.88 ± 0.19	1.09 ± 0.02

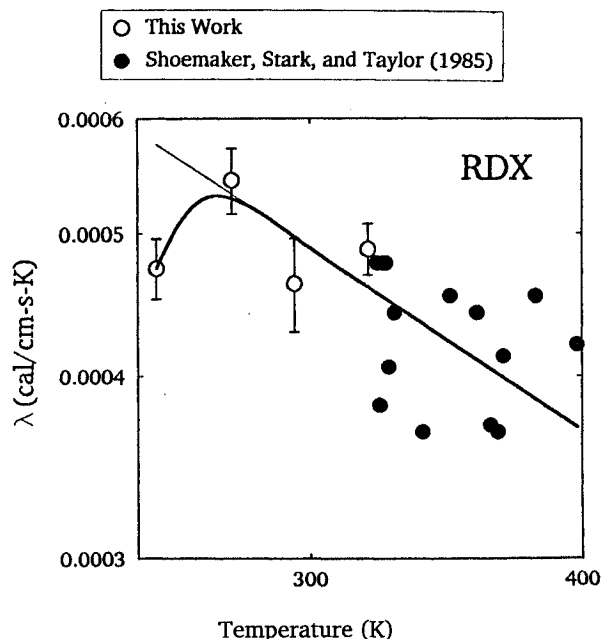


Fig. 1 Thermal conductivity of polycrystalline RDX: open circles—present data; filled circles—data of Shoemaker et al.³; thin line— $0.147/T$; heavy line— $\lambda(T)$ functionality suggested by composite data set (see Discussion section).

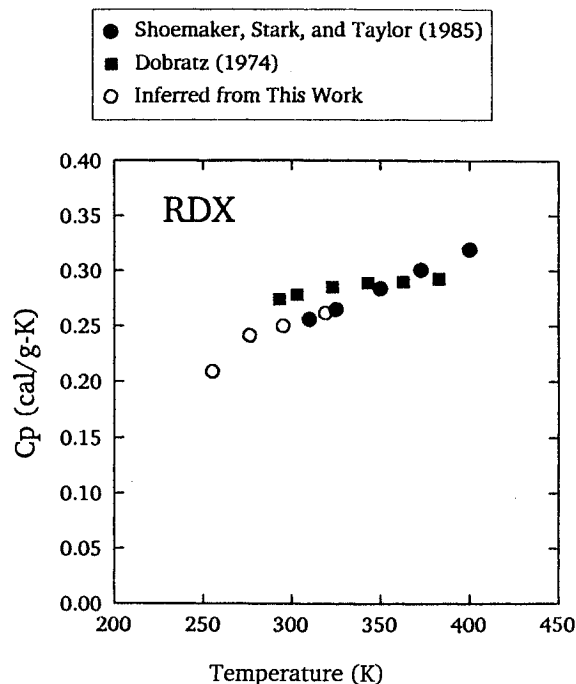


Fig. 2 Specific heat of RDX: filled circles—DSC data of Shoemaker et al.³; filled squares—data from Dobratz⁴; open circles—inferred from present conductivity and diffusivity data.

standard deviations of five experiments at each temperature are given Table 1. All measurements were performed on a single composite specimen. These data may be compared with prior work over a complementary temperature range. Figure 1 shows our data for thermal conductivity along with that of Shoemaker et al.,³ who used a laser-flash method on a pressed-powder specimen. The agreement is good. Another comparison is afforded by measurements of the specific heat using differential scanning calorimetry (DSC), also reported by Shoemaker et al. Utilizing the definition of thermal diffusivity $\alpha = \lambda/(\rho c_p)$, where α is the diffusivity, λ is the thermal conductivity, ρ is the mass density, and c_p is the specific heat, we computed a value for the specific heat from our measured values of conductivity and diffusivity. We assumed a value for the powder density of 1.716 g/cc based on 95% of TMD (1.806 g/cc)⁴ mentioned above. The resulting comparison is shown in Fig. 2 along with the addition of a third set of data given by Dobratz.⁴ The agreement among all three data sets is good. Shoemaker et al. state that military-grade RDX was used in their experiments. This means that up to about 20% of HMX may have existed as an impurity in their test specimens; no chemical analysis was reported by these authors. Also, no information on sample purity was given for the data quoted by Dobratz.⁴

Discussion

According to theory,⁵ the intrinsic thermal conductivity of a dielectric crystalline material, i.e., the conductivity in the absence of lattice imperfections, has a $1/T$ temperature dependence at high temperatures. For this reason the data of Fig. 1 are plotted on a log-log scale, and the thin straight line is a least-squares fit of the function b/T to the combined data sets excluding the point at lowest temperature. The resulting value of b is 0.147 in the units appropriate to the figure. In the low-temperature limit, λ increases with temperature, according to theory.⁵ A peak is thus expected on theoretical grounds in the curve $\lambda(T)$. The line b/T is consistent with the standard deviations of our three highest temperature measurements and the data of Shoemaker et al.³; however, our lowest temperature measurement is almost five standard deviations below the b/T line. We therefore speculate that our data encompasses the maximum in $\lambda(T)$ for RDX, and draw the heavy curved line in Fig. 1 to suggest a functionality consistent with all of the data. Further measurements at still lower temperatures would be desirable to confirm this behavior, but were not possible within the constraints of this work. Interestingly, the value of b obtained from a least-squares fit to the Shoemaker et al. data alone differed from the value obtained from a fit to our data alone (excluding the data at 255 K) by only 0.3%, a fact that is not immediately evident from Fig. 1, but one that adds confidence to the combined-data fit. Finally, we note that the fit, $\lambda(T) = b/T$, found above should provide a reasonable basis for extrapolation up to the melting point 478 K, provided that the application times considered do not permit appreciable thermal decomposition to occur.

References

- Miller, M. S., and Kotlar, A. J., "Technique for Measuring Thermal Diffusivity/Conductivity of Small Thermal-Insulator Specimens," *Review of Scientific Instruments*, Vol. 64, No. 10, 1993, pp. 2954–2960.
- Miller, M. S., "Step-Function Current in a Metallic Foil as a Step-Function Heat-Flux Source," *Journal of Applied Physics*, Vol. 72, No. 9, 1992, pp. 3904–3907.
- Shoemaker, R. L., Stark, J. A., and Taylor, R. E., "Thermophysical Properties of Propellants," *High Temperatures—High Pressures*, Vol. 17, 1985, pp. 429–435.
- Dobratz, B. M., "Properties of Chemical Explosives and Explosive Simulants," Lawrence Livermore Lab., UCRL-51319 REV. 1, Livermore, CA, July 1974.
- Klemens, P. G., "Theory of the Thermal Conductivity of Solids," *Thermal Conductivity*, edited by R. P. Tye, 1st ed., Vol. 1, Academic Press, New York, 1969, Chap. 1.

Non-Darcy Mixed Convection in a Vertical Porous Channel with Asymmetric Wall Heating

H. A. Hadim* and G. Chen†
Stevens Institute of Technology,
Hoboken, New Jersey 07030

Nomenclature

C	= inertia coefficient
Da	= Darcy number, K/W^2
Gr^*	= modified Grashof number, $(g\beta TKW)/\nu^2$ or $(g\beta q_2 KW^2)/(\nu^2 k)$
g	= acceleration of gravity
h	= heat transfer coefficient
K	= permeability of the porous medium
k	= thermal conductivity
Nu	= local Nusselt number
Pe	= Peclet number
Pr	= Prandtl number
q	= heat flux
Re	= Reynolds number
r_{11}	= ratio of wall heat fluxes, q_1/q_2
r_T	= ratio of wall temperature difference, $(T_1 - T_0)/(T_2 - T_0)$
T	= temperature
U	= dimensionless velocity in x direction
V	= dimensionless velocity in y direction
\mathbf{V}	= velocity vector
V_0	= uniform inlet velocity
W	= channel width
X	= dimensionless distance in horizontal x direction
Y	= dimensionless distance in vertical y direction
β	= thermal expansion coefficient of the fluid
ε	= porosity
ζ	= vorticity, $\partial V/\partial X - \partial U/\partial Y$
θ	= dimensionless temperature, $(T - T_0)/(T_2 - T_0)$ or $(T - T_0)/(q_2 W/k)$
ν	= kinematic viscosity
ψ	= stream function

Introduction

RECENTLY, fundamental studies of thermal convection in fluid-saturated porous media have generated significant interest due to their diverse engineering applications, including geothermal systems, building thermal insulation, enhanced oil recovery methods, nuclear waste disposal, packed-bed chemical reactors, and solid-matrix heat exchangers. Recent comprehensive reviews of convective transport in porous media are provided by Kakac et al.¹ and Nield and Bejan.²

As indicated by Hadim,³ relatively few investigations have been conducted on mixed convection in vertical porous channels, and most of them were limited to the Darcy flow regime. In the present study, a detailed numerical investigation of mixed convection in a vertical porous channel heated asymmetrically at the walls is performed with particular emphasis on the developing region. Both uniform wall temperature (UWT) and uniform wall heat flux (UHF) conditions are examined for the case when buoyancy effects are assisting the "upward" flow.

Received Oct. 18, 1993; revision received May 3, 1994; accepted for publication May 13, 1994. Copyright © 1994 by the American Institute of Aeronautics and Astronautics, Inc. All rights reserved.

*Associate Professor, Department of Mechanical Engineering.

†Graduate Research Assistant, Department of Mechanical Engineering.